Pseudo-static analysis of inclined pile foundations in OpenSees

Yu (Yuri) Wang

Geotechnical Engineer, Engineering Geology Ltd

PhD, University of Auckland

27/01/2022

1. Introduction

- Inclined piles (or raked/batter piles) have been frequently applied to provide substantial lateral stiffness for underground structures, bridges, offshore structures, etc.

- The advantages of inclined piles remarked in the literature include resisting lateral spreading in liquefiable ground, and reduction in the horizontal cap displacement, overturning moment, base shear force and total bending moment of piles.

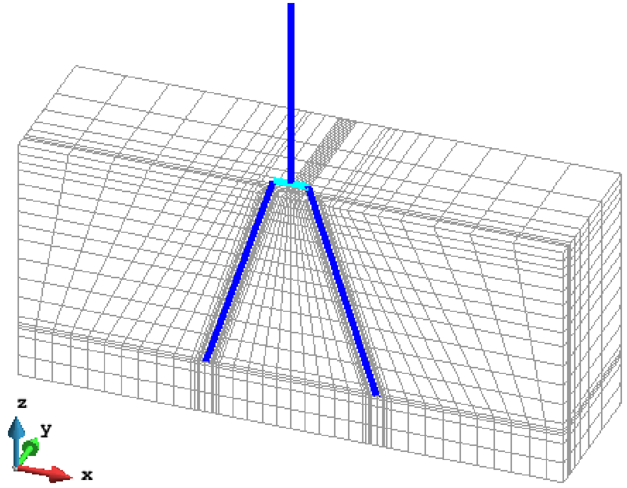

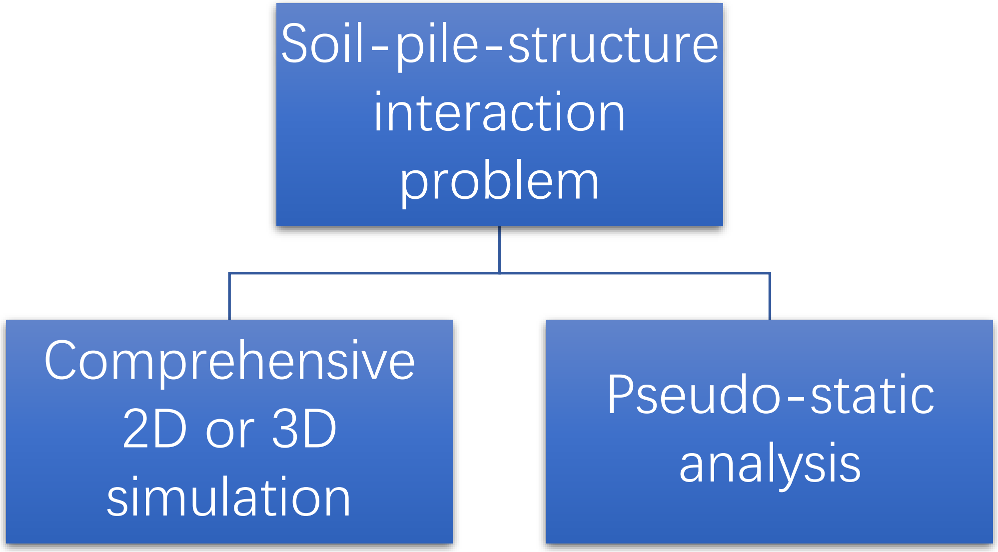

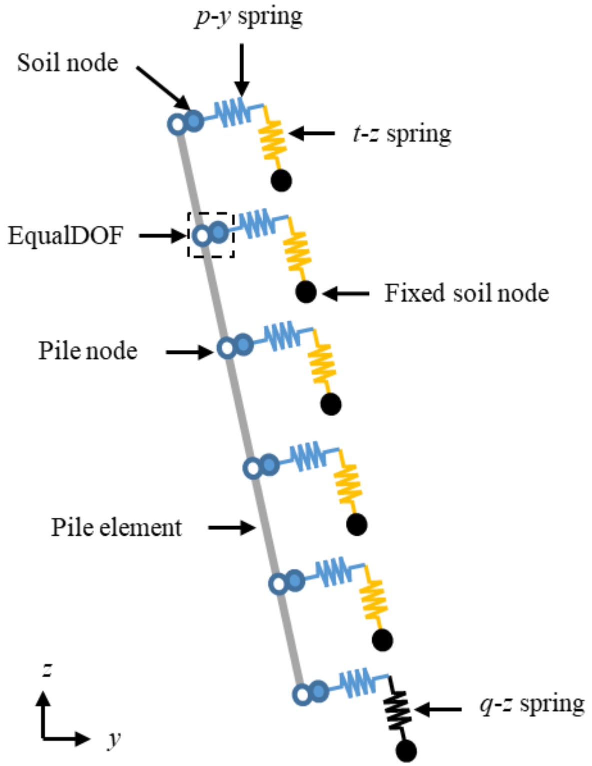

1. Introduction

- A review of the literature shows some findings in terms of the bearing, pull-out, and shear capacity of inclined piles:
    - Lateral resistance: negative inclined piles > vertical piles > positive inclined piles;
    - Vertical bearing capacity: increases with increasing pile inclination and decreases after attaining the maximum value at around 15° to 20°.
    - Pull-out capacity: both decreases and increases were observed.

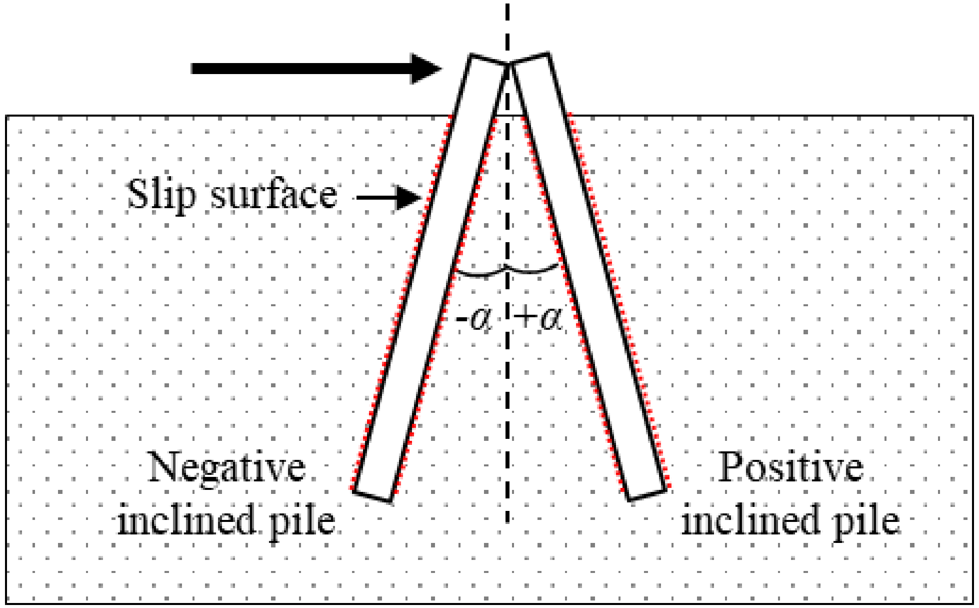

Definition of negative and positive inclined piles: a positive inclined pile has a slip surface deflecting upward, while the slip surface of a negative batter pile deflects downward

2. Methodology

Analysis procedure

Parametric analysis based on 3D FEM models → Modification of spring parameters for inclined pile → Construction of the pseudo-static method

FEM scheme

Range of investigated parameters

Parameters	Range
Pile inclination, *α*	0°, 5°, 10°, 15°, 20°, 25°, and 30°
Pile type	XS, S, M, and L
Relative density of soil, *Dr*	33%, 55%, and 80%
Loading pattern	Axial bearing, axial pull-out, positive shear, and negative shear loadings

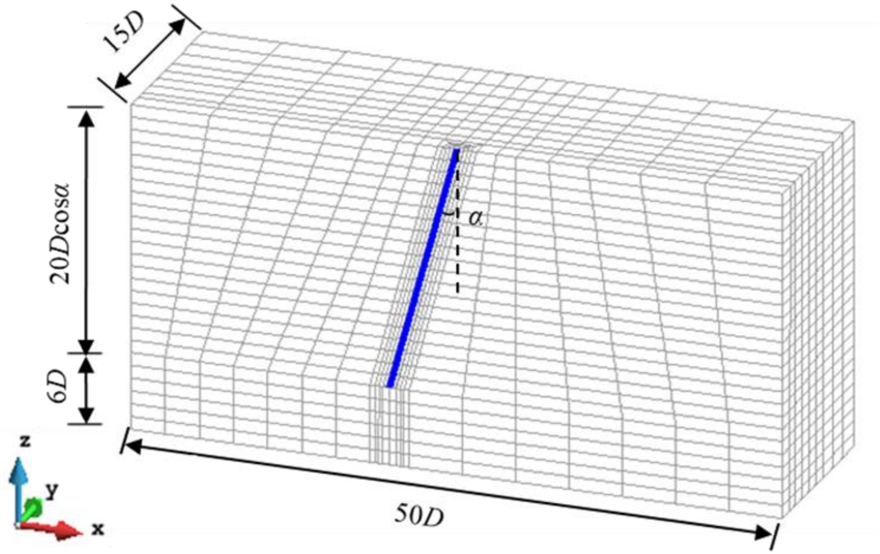

Layout of the 3D FEM model used in the analysis.

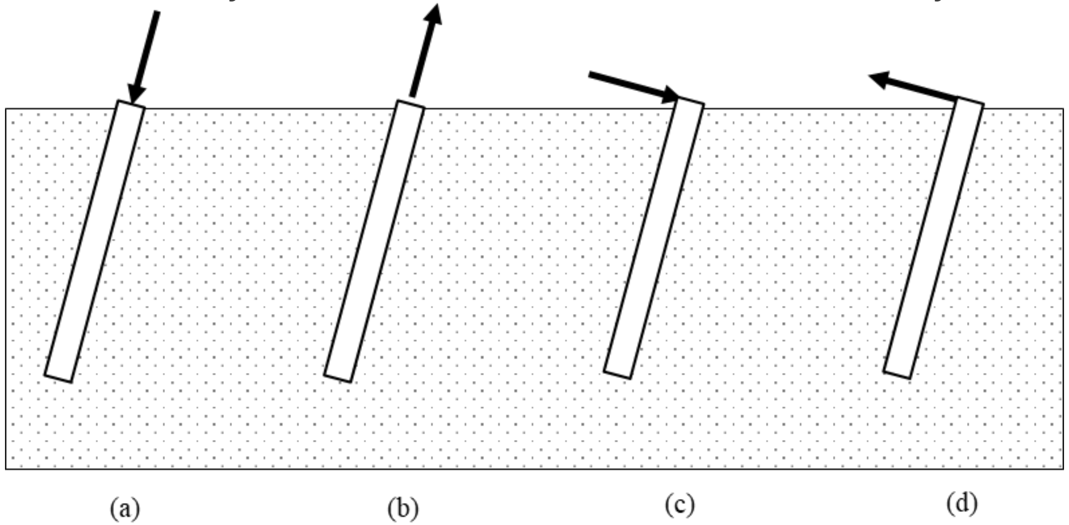

Loading patterns: (a) axial bearing; (b) axial pull-out; (c) negative shear; and (d) positive shear.

2. Methodology

Soil Simulation

Pressure-Dependent Multi-Yield Surface Model (PDMY02):
- Parameters are from Khosravifar et al. (2014).

Pile Simulation

Hybrid element:
- Beam elements for the pile: simple and convenient to obtain the internal forces in the pile;
- Stiff beam elements for the pile skeleton: capture the pile geometry more like the actual case.

Soil-Pile Interface

Zero-length flat slider bearing element:
- Separation;
- Friction (Coulomb friction law):
  - Friction coefficient: $\mu = \tan(2\varphi_f/3)$
  - Normal and tangential stiffnesses: $K_N = K_T = 1.0\times10^7\ kPa$

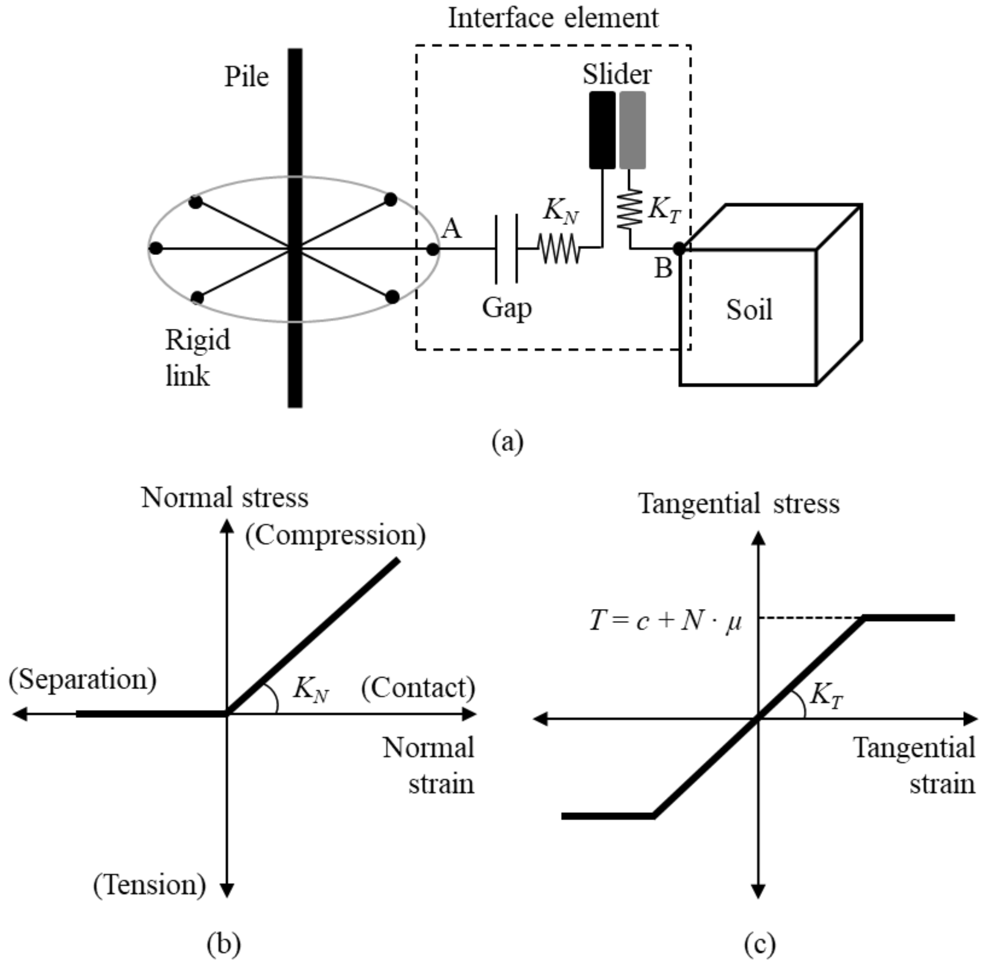

Simulation of the pile and interface: (a) beam element method; (b) solid element method; and (c) hybrid element method.

3. 3D Simulation Results

The impact of pile inclination on the ultimate capacities is expressed quantitatively in terms of performance index P (in percentage):

$$P = \frac{Q_I - Q_V}{Q_V} \times 100\%$$

where Q_I and Q_V are the calculated quantities (i.e., ultimate capacities) for inclined and vertical pile configurations, respectively.

Axial demand

- Obtain a series of load-displacement curves.
- Calculate the performance index of axial capacity.
- Find the relationship between the performance index and investigated parameters.

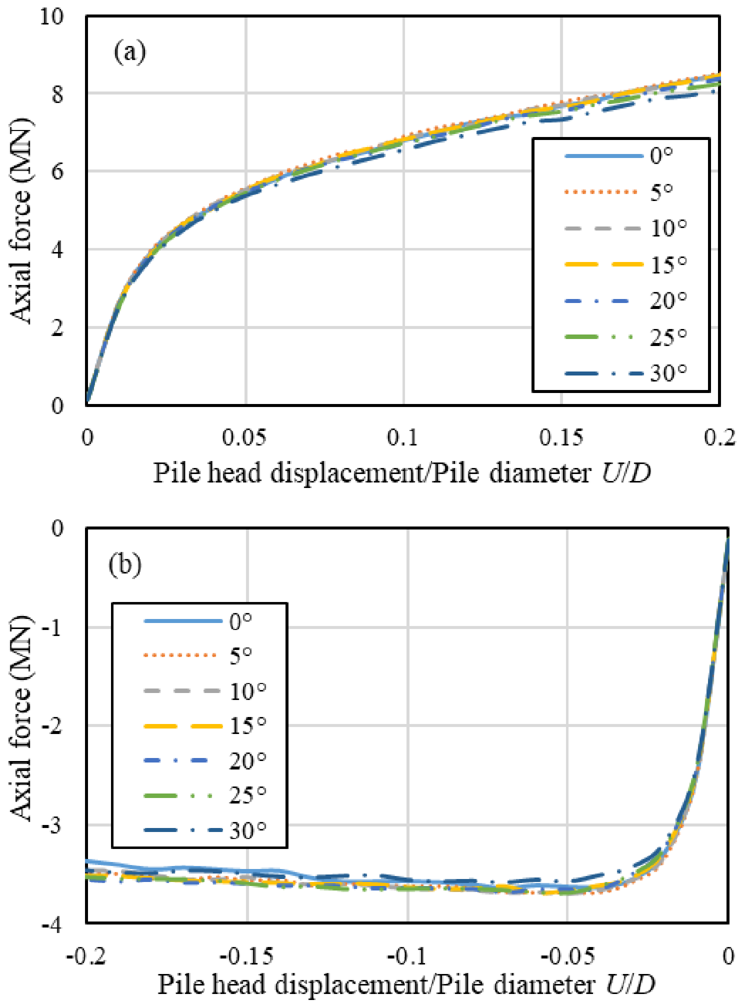

Axial load-displacement curves for small piles with different inclinations in medium-dense sand: (a) bearing capacity; and (b) pull-out capacity.

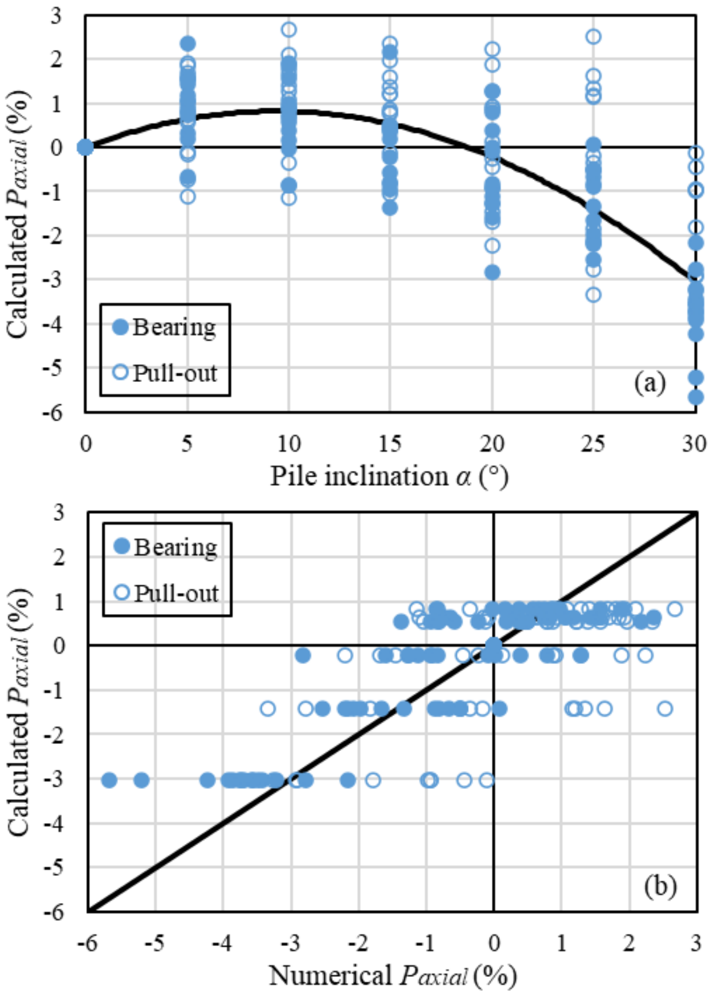

Performance indices for the axially-loaded piles investigated in this study: (a) bearing capacity; and (b) pull-out capacity.

3. 3D Simulation Results

Axial demand

No obvious impacts of pile size and soil relative density were detected. The influence of the pile inclination on the axial demand (performance index) is related to pile inclination only:

$$P_{axial} = \cos(0.55\alpha)[\cos(0.55\alpha)+0.1\alpha]-1 \quad (\alpha \text{ in radian})$$

Other formulas:

- Li et al. (2018)

$$P_b = \cos(1.35\alpha)-1$$

- Hanna & Afram (1986)

$$P_p = \cos(0.5\alpha)-1$$

- Nazir & Nasr (2013)

$$P_p = \cos\alpha\left(\cos\alpha + 2/3\alpha\right)-1$$

The proposed curve generally plots as a compromise between the experimental data and other available equations in the literature.

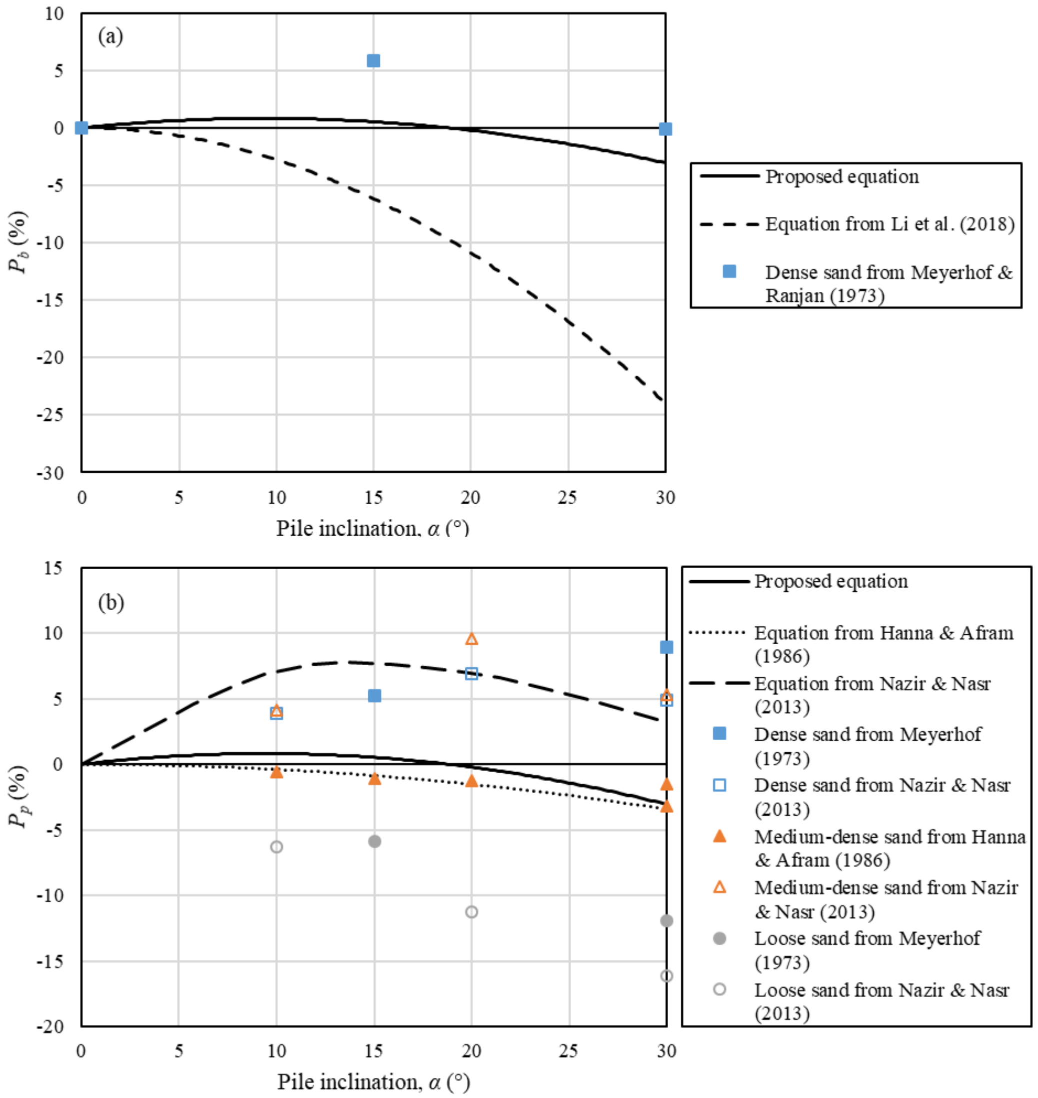

Comparison between predicted and experimental indices:
(a) bearing capacity; and (b) pull-out capacity.

3. 3D Simulation Results

Shear demand

The performance index for negative and positive shear demands P_{s-} or P_{s+} can be expressed as

$$P_s = f(Dr)\, f\left(\frac{E_p I_p}{E_s D^4}\right) f(\alpha)$$

where E_pI_p/E_sD^4 is the stiffness ratio of pile and soil.

- Step 1: $f(\alpha)$ - Plot P_s vs α relationships by fixing Dr and E_pI_p/E_sD^4
- Step 2: $f(E_pI_p/E_sD^4)$ - take the slopes of P_s-α relationships as the value of $f(E_pI_p/E_sD^4)$.
- Step 3: *f(Dr)* - calculate *f(Dr)* by using the two formulas.

Final shear demands:

$$P_s = \begin{cases} (7.16Dr + 1.04)\left[\ln\left(\frac{E_p I_p}{E_s D^4}\right) - 13.6\right]\sin\alpha, & -25° < \alpha < 0° \\ -(51.13Dr + 16.14)\sin\alpha, & 0° < \alpha < 25° \end{cases}$$

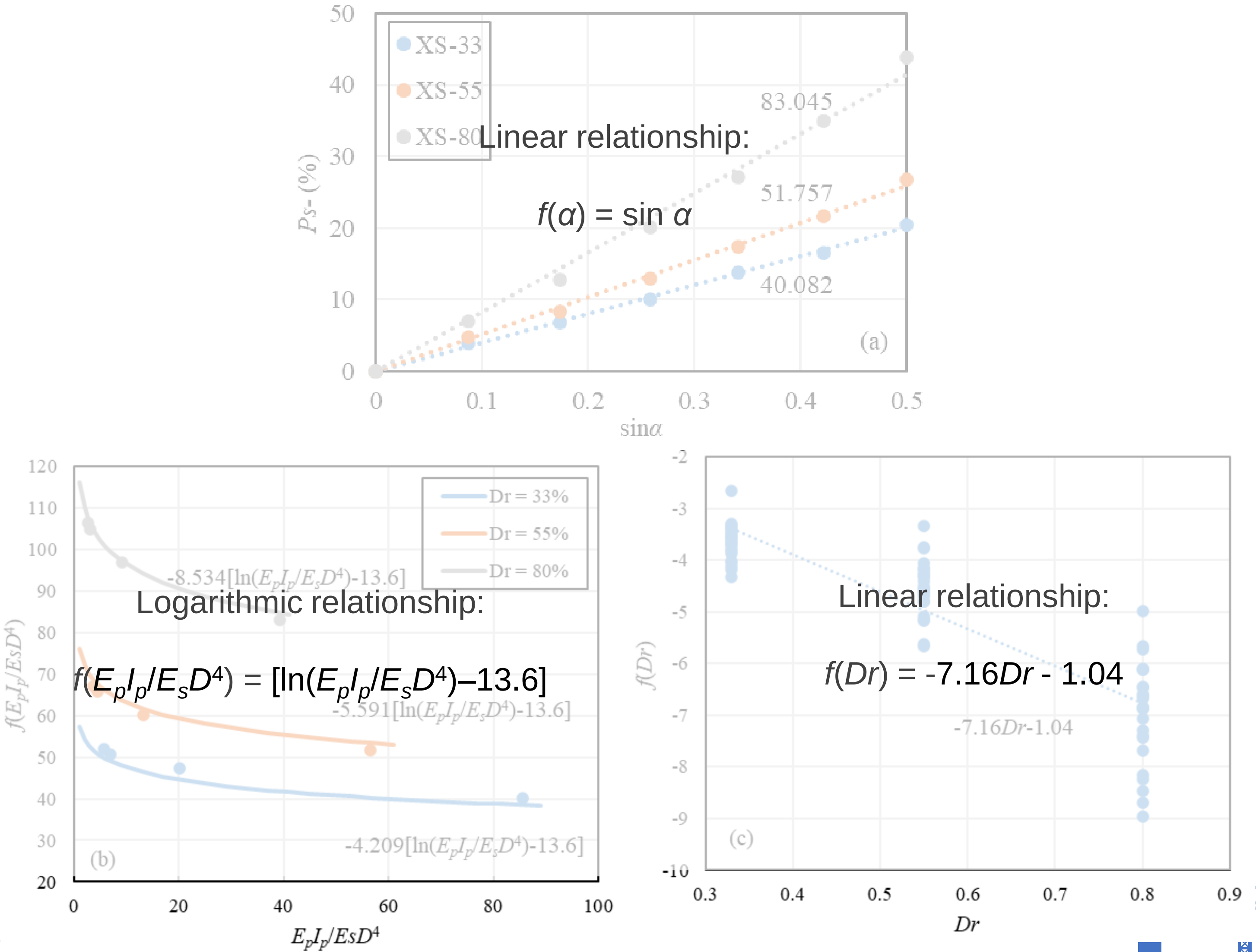

Influences of various factors on the negative shear demands: (a) pile inclination; (b) stiffness ratio of pile and soil; and (c) relative density of sand.

3. 3D Simulation Results

Shear demand

The performance index for negative and positive shear demands P_{s-} or P_{s+} can be expressed as

$$P_s = f(Dr)\, f\left(\frac{E_p I_p}{E_s D^4}\right) f(\alpha)$$

where E_pI_p/E_sD^4 is the stiffness ratio of pile and soil.

- Step 1: $f(\alpha)$ - Plot P_s vs α relationships by fixing Dr and E_pI_p/E_sD^4
- Step 2: $f(E_pI_p/E_sD^4)$ - take the slopes of P_s-α relationships as the value of $f(E_pI_p/E_sD^4)$.
- Step 3: $f(Dr)$ - calculate $f(Dr)$ by using the two formulas.

Final shear demands:

$$P_s = \begin{cases} (7.16Dr + 1.04)\left[\ln\left(\frac{E_p I_p}{E_s D^4}\right) - 13.6\right]\sin\alpha, & -25° < \alpha < 0° \\ -(51.13Dr + 16.14)\sin\alpha, & 0° < \alpha < 25° \end{cases}$$

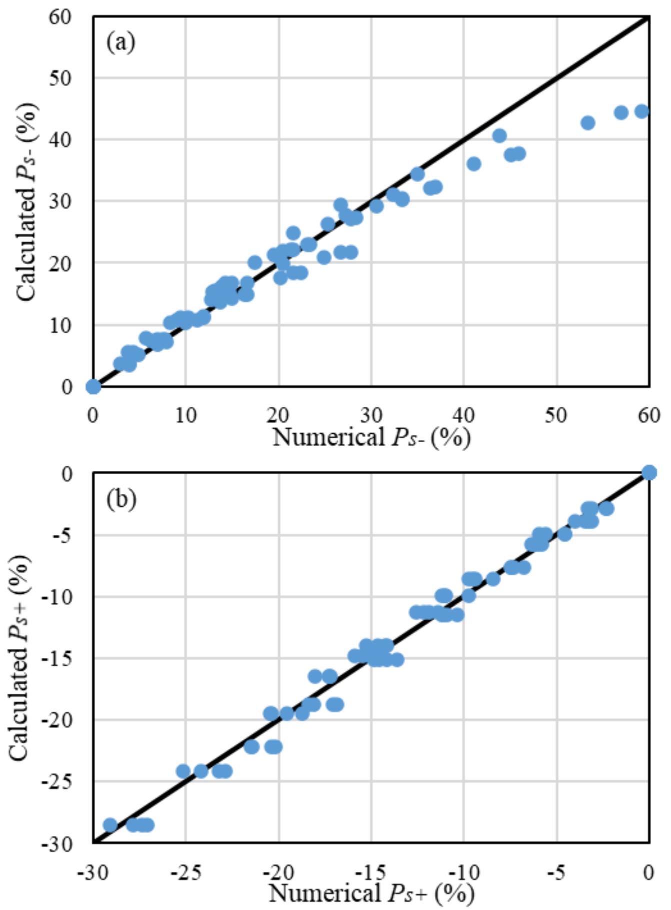

Influences of various factors on the negative shear demands: (a) pile inclination; (b) stiffness ratio of pile and soil; and (c) relative density of sand.

4. Pseudo-static analysis

Implementation of the pseudo-static method

Three types of springs (i.e., *p–y*, *t–z*, and *q–z* springs) adopted in the pseudo-static analysis are given as (API, 2007; Mosher & Dawkins, 2000; Vijayvergiya, 1977):

$$p(y) = p_u \tanh\left(\frac{k_T}{p_u} y\right)$$

$$t(z) = \frac{z}{(1/k_f) + (z/t_u)}$$

$$q(z) = q_u \left(\frac{z}{z_c}\right)^{1/3}$$

The inputs for the three spring materials are the **ultimate resistance** and the displacement when 50% of the ultimate resistance is mobilized in monotonic loading:

$$y_{50} = \frac{p_u}{k_T} \tanh^{-1}(0.5)$$

$$z_{50} = \frac{t_u}{k_f}, \text{ for } t-z \text{ curves}$$

$$z_{50} = 0.125 z_c, \text{ for } q-z \text{ curves}$$

$$\frac{q_u^{inclined}}{q_u^{vertical}} = \frac{t_u^{inclined}}{t_u^{vertical}} = \frac{k_f^{inclined}}{k_f^{vertical}} = P_{axial} + 1$$

$$\frac{p_u^{inclined}}{p_u^{vertical}} = \frac{k_T^{inclined}}{k_T^{vertical}} = P_s + 1$$

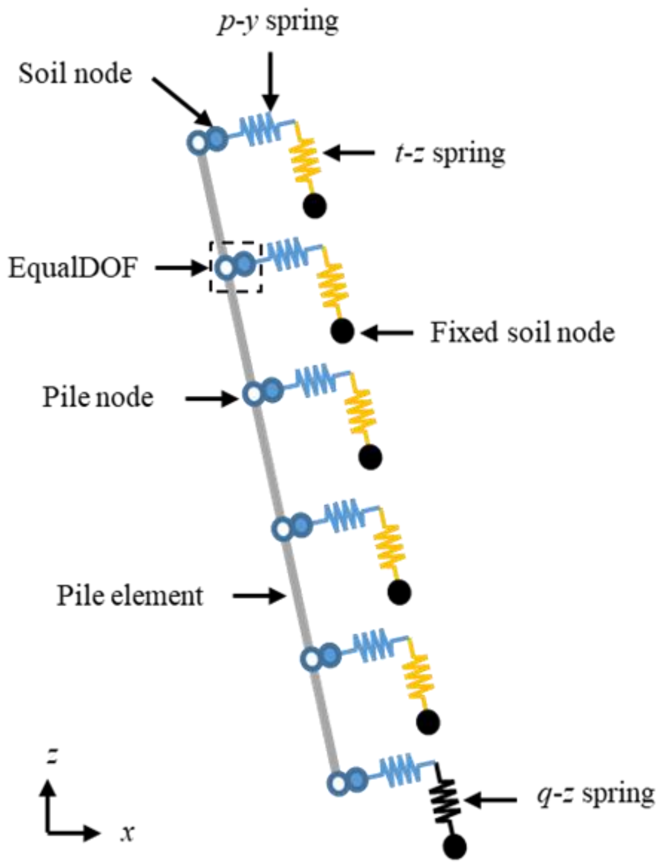

Definition of the pseudo-static model in OpenSees.

4. Pseudo-static analysis

Case Study 1: 3D FEM analysis

The seismic performance of a 1 × 2 pile group embedded in liquefiable sands was simulated by using both the 3D FEM approach and the proposed pseudo-static approach (β = 4°, α = 0° ~ 25°).

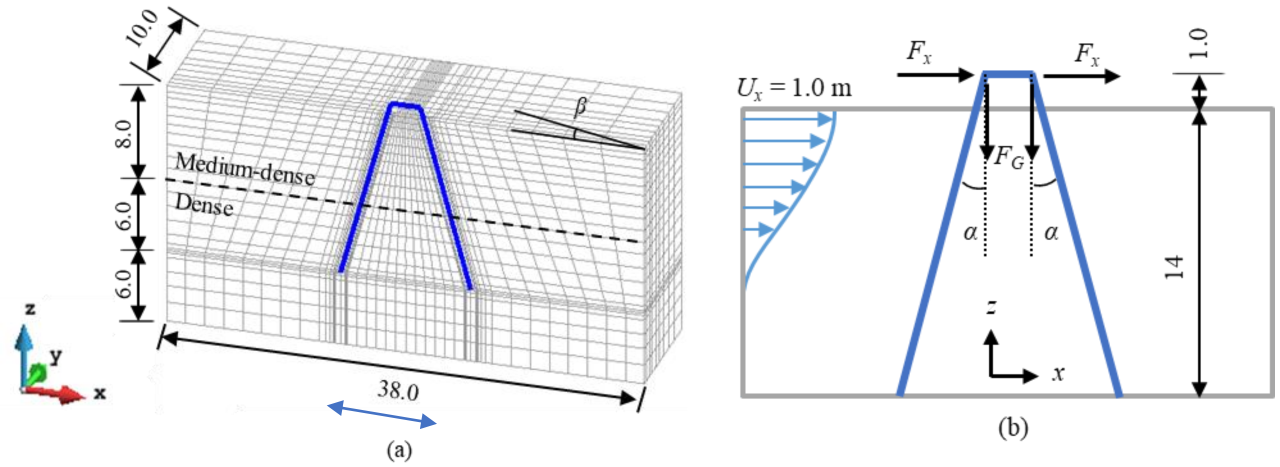

Schematic of the numerical model in Case Study 1 (in meter): (a) 3D FEM model; and (b) pseudo-static model.

Compared with the 3D FEM analysis, the pseudo-static analysis saves high computational costs and yet reproduces the inertial forces and lateral displacement of inclined piles in 3D FEM analysis with reasonable accuracy.

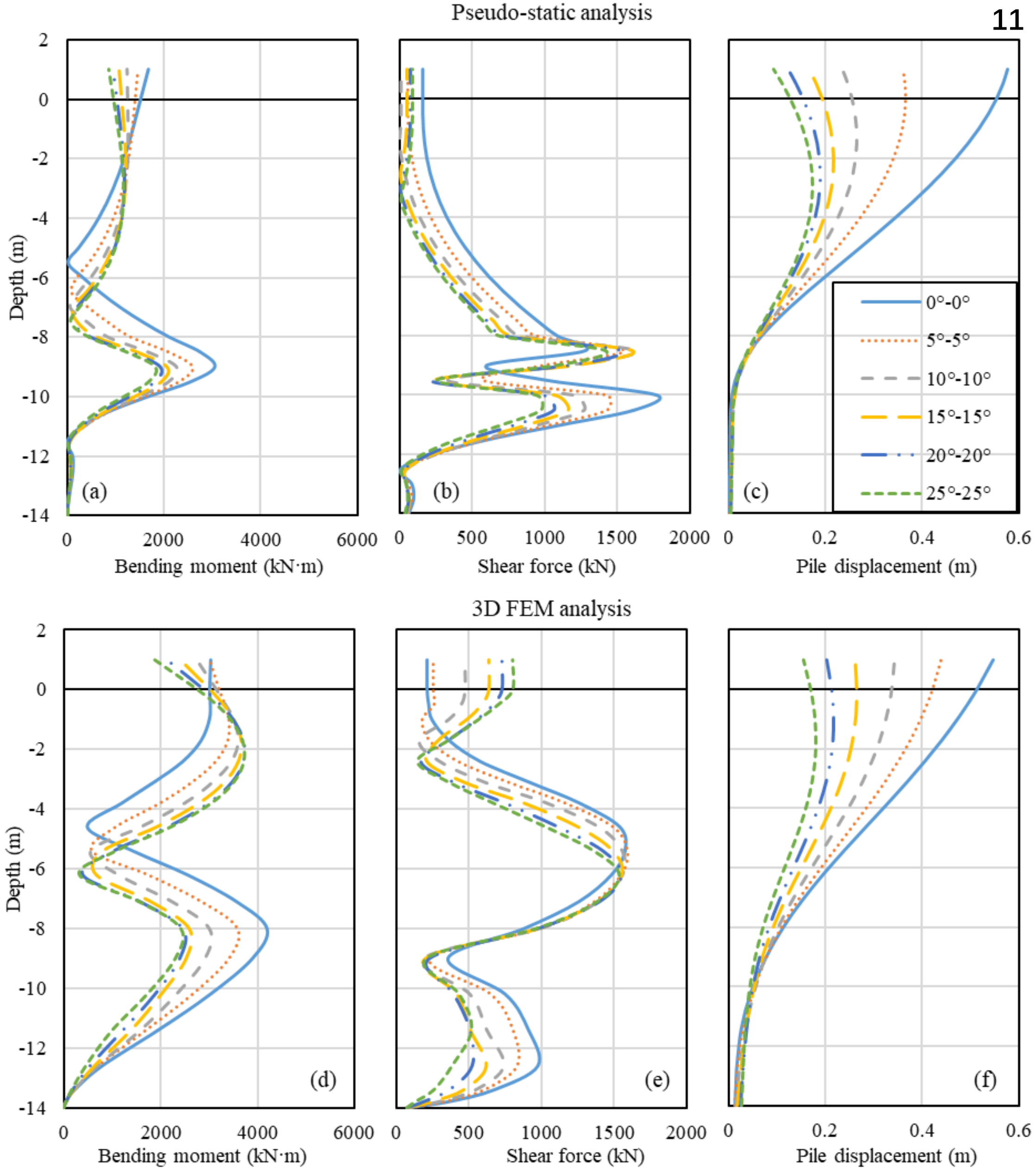

Comparison between numerical results for Case Study 1

4. Pseudo-static analysis

Case Study 2: Centrifuge experiment

A centrifuge experiment by Li et al. (2016) has been simulated by both the 3D FEM approach and the proposed pseudo-static approach.

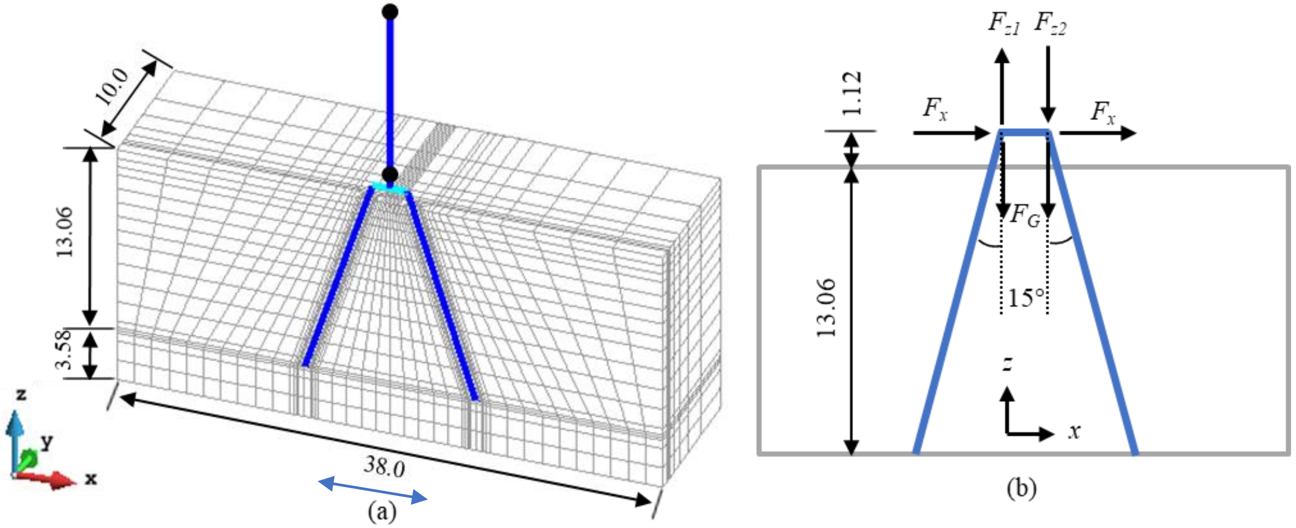

Schematic of the numerical model in Case Study 2 (in meter): (a) 3D FEM model; and (b) pseudo-static model.

The proposed pseudo-static method can provide a reasonable assessment of the peak axial compression forces and bending moments of piles.

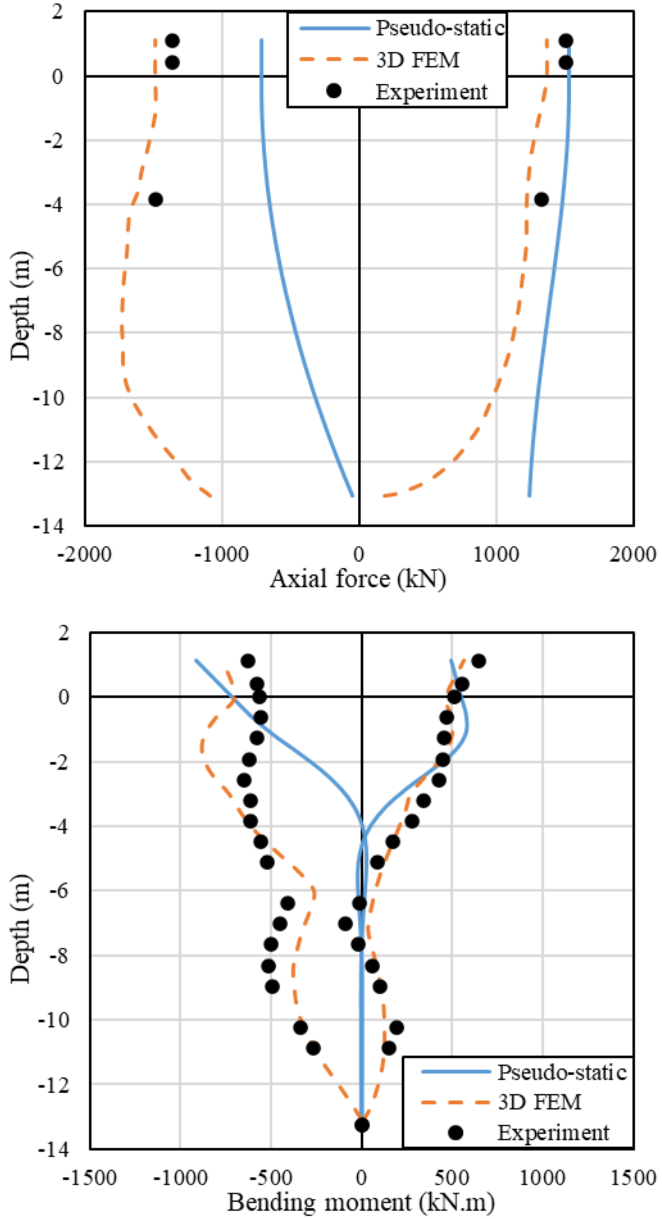

Results comparison for Case Study 2

4. Pseudo-static analysis

Case Study 3: Field performance

The Landing Road Bridge in Whakatane, New Zealand, was subjected to significant lateral spreading during the 1987 Edgecumbe earthquake.

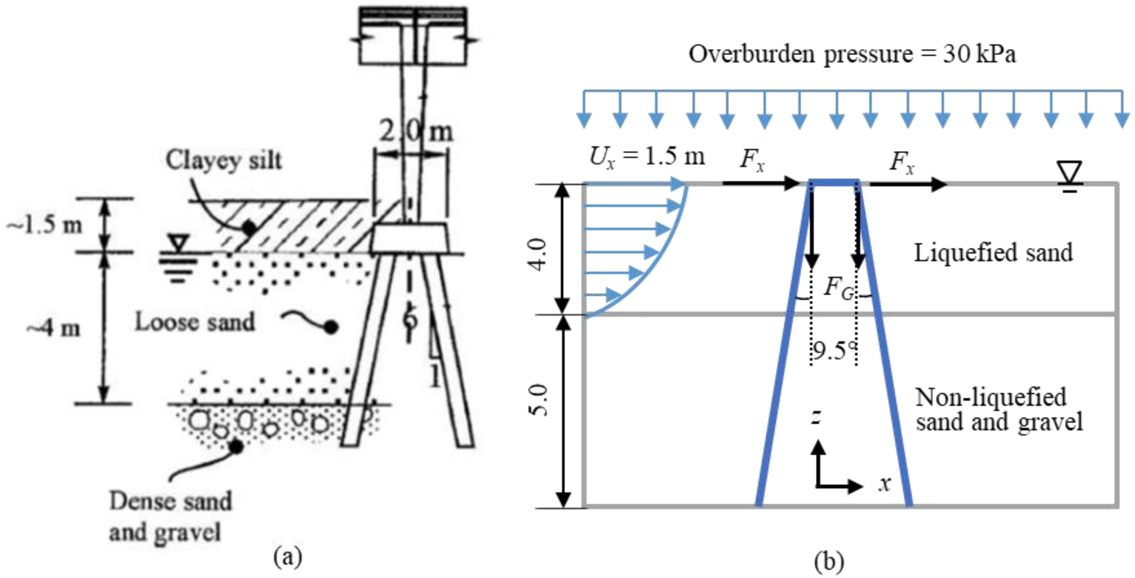

Schematic of the numerical model in Case Study 3: (a) details of the investigated foundation of Landing Road Bridge (from Yasuda & Berrill, 2000); and (b) pseudo-static model.

The numerical results from the pseudo-static analysis appear to coincide with the field observations (minor cracking was observed at the pile heads).

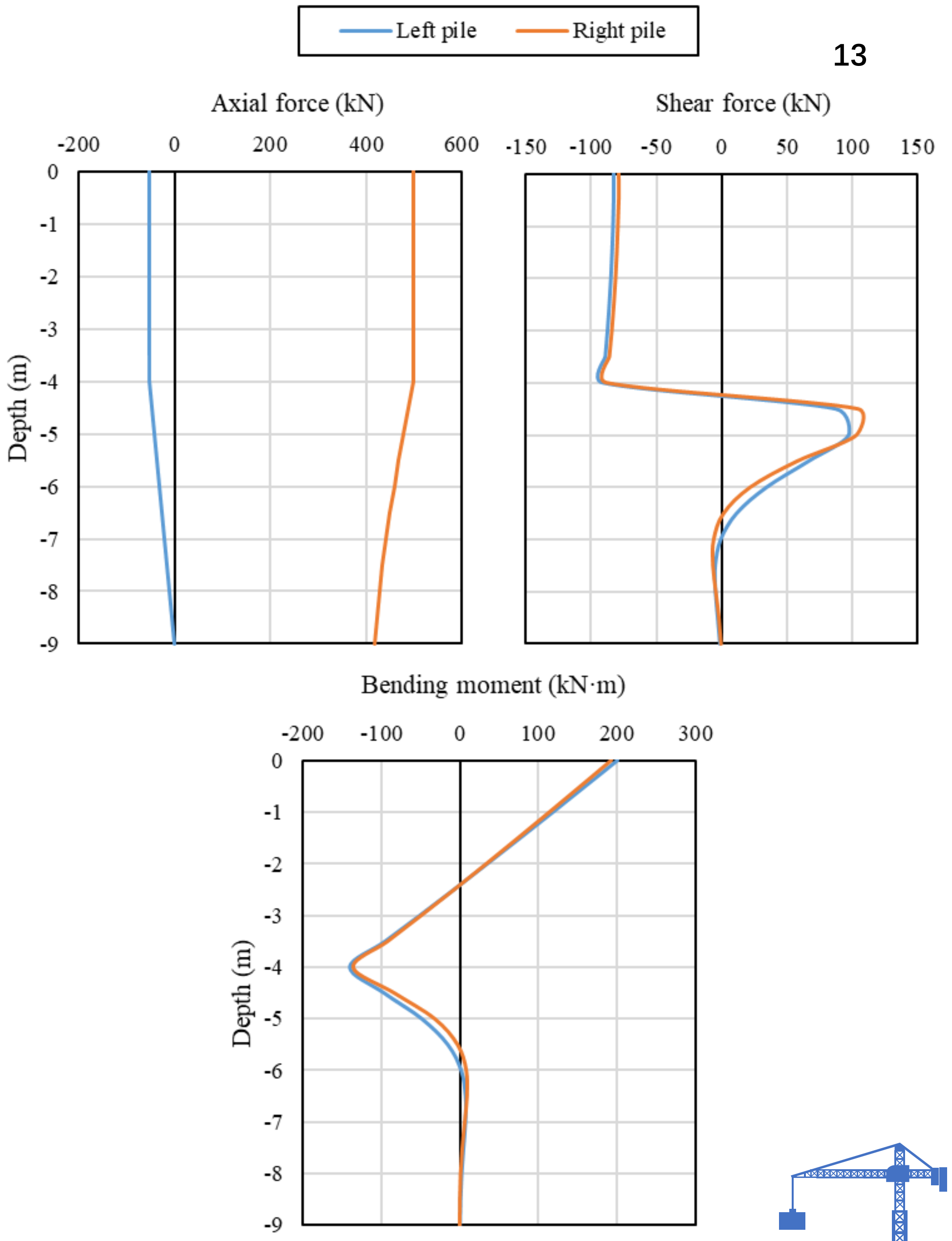

Response of inclined piles of the Landing Road Bridge

5. Concluding remarks

- This research employed the 3D FEM analyses to investigate the axial and shear behavior of inclined piles. The axial bearing, axial pull-out, negative shear, and positive shear capacities were investigated. Relationships of the capacities between the inclined and vertical piles were directly related to the pile inclination, soil relative density, and stiffness ratio of the pile and the soil through the proposed equations.

$$P_{axial} = \cos(0.55\alpha)[\cos(0.55\alpha) + 0.1\alpha] - 1 \quad (\alpha \text{ in radian})$$

$$P_s = \begin{cases} (7.16Dr + 1.04)\left[\ln\left(\dfrac{E_p I_p}{E_s D^4}\right) - 13.6\right]\sin\alpha, & -25^\circ < \alpha < 0^\circ \\ -(51.13Dr + 16.14)\sin\alpha, & 0^\circ < \alpha < 25^\circ \end{cases}$$

- The pseudo-static analysis for inclined piles has been proposed and validated by using different case studies. The pseudo-static method using the modified soil springs for inclined piles produced acceptable predictions of axial forces and bending moments that compared well with 3D FEM results, experimental results, and field observations.

Thank You!
Questions?

References

- API. (2007) Recommended Practice for Planning, Designing and Constructing Fixed Offshore Platforms - Working Stress Design, API Recommended Practice.
- Hanna, A. M. & Afram, A. (1986). Pullout capacity of single batter piles in sand. Canadian Geotechnical Journal, 23(3), 387–392.
- Li, Z., Escoffier, S., & Kotronis, P. (2016). Centrifuge modeling of batter pile foundations under sinusoidal dynamic excitation. Bulletin of Earthquake Engineering, 14(3), 673–697.
- Li, Z., Kotronis, P., Escoffier, S., & Tamagnini, C. (2018). A hypoplastic macroelement formulation for single batter piles in sand. International Journal for Numerical and Analytical Methods in Geomechanics, 42(12), 1346–1365.
- Khosravifar, A., Boulanger, R. W., & Kunnath, S. K. (2014). Design of extended pile shafts for the effects of liquefaction. Earthquake Spectra, 30(4), 1775–1799.
- Mosher, R. L. & Dawkins, W. P. (2000). Theoretical Manual for Pile Foundations. Washington, D.C.: US Army Corps of Engineers, Engineer Research and Development Center.
- Nazir, A. & Nasr, A. (2013). Pullout capacity of batter pile in sand. Journal of Advanced Research, 4(2), 147–154.
- Vijayvergiya, V. N. (1977). Load-movement characteristics of piles. In Proceeding of Ports 77 Conference. New York: ASCE.
- Yasuda, I. S. & Berrill, J. B. (2000). Observations of the earthquake response of foundations in soil profiles containing saturated sands. In Proceedings of the GeoEng 2000 Conference. Melbourne, Australia.